Analysis of Effective Impedance Transmitted to the Operator in Position-Exchange Bilateral Teleoperation

Nick Colonnese[1] and Allison M. Okamura[2]

***Abstract*—In this paper, we analyze the impedance transmitted to the operator in position-exchange bilateral teleoperation including the effects of master and slave dynamics, local and communication time delay, low-pass filtering of the velocity estimate, and controller stiffness and damping, for three different environment dynamics: free, clamped, and a mass-damper-spring. We show the impedance transmitted the operator numerically using effective impedances, a conceptual tool that decomposes the impedance into components with physical analogs, and also present symbolic expressions for the effective stiffness and damping transmitted to the operator at low frequencies. Our results show that local and communication time delay do not significantly affect the effective stiffness, strongly affect effective damping, and weakly affect effective mass transmitted to the operator. The low-pass filter cut-off frequency affects the impedance transmitted to the operator differently depending on the environment impedance. For many cases, increasing the cutoff frequency primarily increases the effective damping bandwidth. Increasing controller stiffness increases the effective stiffness transmitted to the operator at low frequencies, but can significantly change the effective stiffness, damping, and mass, at higher frequencies. Experimental data gathered using a bilateral telemanipulator consisting of two Phantom Premium 1.5 robots interacting with a custom-made environment validates the theoretical analysis.**

I. Introduction

Bilateral teleoperators allow a human operator interact with an environment through a robot that provides force feedback. For many teleoperation applications, such as medical or rehabilitation procedures, impedance-type master and slave robots driven by force source actuators, e.g., dc motors, are controlled using an impedance-impedance control architecture (see Figure 1).

An ideal teleoperator is perfectly *transparent*, meaning that the impedance transmitted to the operator is exactly the impedance of the environment, i.e., the teleoperator would feature force feedback as if the operator was interacting with the environment directly. Transparent teleoperators should feel exactly as desired, with no unwanted effects from a multitude of sources such as master or slave dynamics (i.e., inherent mass and damping), the controller virtually linking the master and slave, low-pass filtering to mitigate noise, or time delay. In practical teleoperation scenarios, perfect transparency cannot be achieved, and it can be difficult to predict and interpret how the parameters of the teleoperator affect the dynamics transmitted to the operator using conventional analysis tools. For example, a Bode plot cannot directly describe how a teleoperator with significant communication time delay will feel compared to one with no delay. Similarly, the Z-width cannot directly predict what master-slave tracking performance is necessary to accurately display the mass of an environment to a human operator. Characterization of the effect of system parameters on how a teleoperator *feels* would be a valuable tool in teleoperator design.

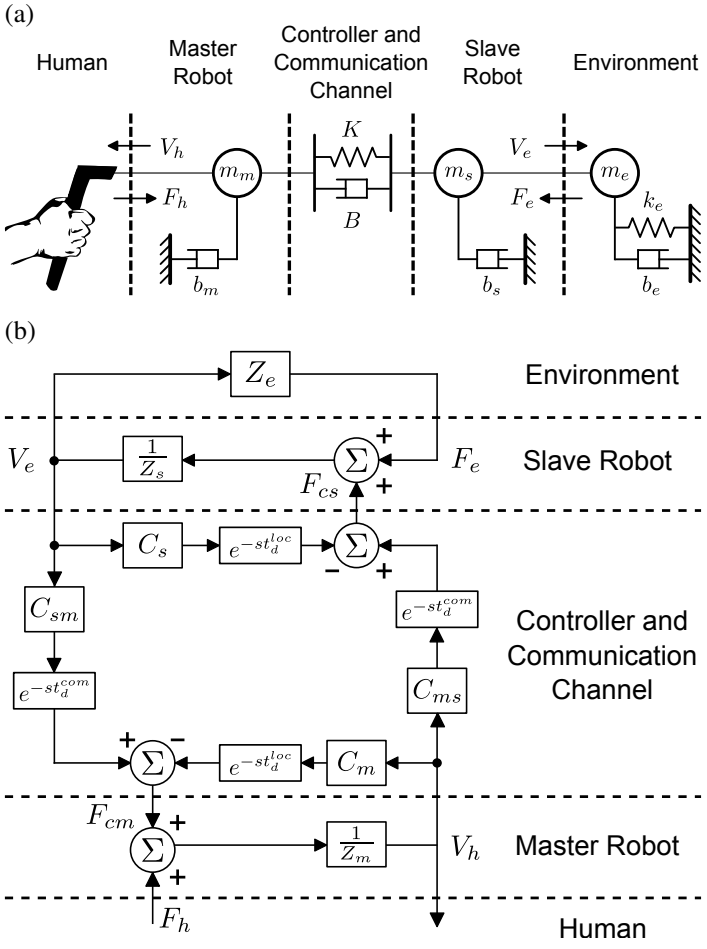

Fig. 1. (a) Schematic of a human operator interacting with an environment through a teleoperator. (b) Block diagram for an impedance-impedance type teleoperator with local time delay, t_d^{loc}, and communication time delay, t_d^{com}. In this paper we consider a simple proportional derivative controller: $C_m = C_s = C_{ms} = C_{sm} = \frac{K}{s} + \left(\frac{\omega_0}{s+\omega_0}\right)B$.

A. Prior Work

This work builds on previous research analyzing the effect of system parameters on the impedance transmitted to the operator.

*This work was supported in part by National Science Foundation grant 1217635

[1]Oculus Research, Redmond, Washington 98052. nick.colonnese@oculus.com

[2]Department of Mechanical Engineering, Stanford University, Stanford, California 94305. aokamura@stanford.edu

Lawrence [6] showed that it is possible for the operator to feel exactly the dynamics of the environment (i.e., achieve perfect transparency), in four channel control architectures (where both position and force of the master and slave are exchanged) for no local or communication time delay. However, because of dynamic uncertainty, necessary local and communication time delay, and desired stability margins, perfect transparency is not attainable in practice.

Hashtrudi-Zaad and Salcudean [5] analyzed the impedance transmitted to the operator numerically using Bode plots at the extremes of the environment impedance: the slave robot in free motion, and the slave robot rigidly clamped to the environment. They found that a decrease in local feedback enhances performance in free motion and the high transparency bandwidth, but reduces stability robustness.

Christiansson and van der Helm [2] analyzed the effects of controller architectures and communication time delay on the transparency of a bilateral teleoperator with a built-in slave-side intrinsic stiffness. They analyzed transparency numerically in terms of "teleoperator stiffness" and "teleoperator damping," scalar characterizations of the impedance transmitted to the operator at low frequencies for specific environment conditions.

Willaert et al. [8] analyzed the effects of modeling error and communication time delay on a bilateral teleoperator using various control architectures. They analyzed transparency symbolically in terms of "stiffness transparency," a scalar characterization of the impedance transmitted to the operator at low frequencies for a pure stiffness environment.

In our previous work [3], we analyzed the closed-loop dynamics of haptic displays in terms of effective impedances. We use a similar approach in this paper, but expand it to consider a bilateral teleoperator instead of a haptic display. This work is significantly more complex than the haptic display case because of the larger number of parameters affecting the operator impedance.

B. Contributions

In this paper, we analyze the impedance transmitted to the operator including the effects of master and slave dynamics, local and communication time delay, the cut-off frequency of the low-pass filter for the velocity estimate, and controller stiffness and damping. We consider three environments: free (the slave robot is not in contact with the environment), clamped (the slave robot is rigidly fixed to the environment), and a mass-damper-spring.

With the aim of intuitively presenting how teleoperator system parameters influence how a teleoperator "feels," we use two different methods. Our first method shows the impedance transmitted to the human operator numerically using effective impedances. Effective impedances are a conceptual tool that decompose an impedance into components with physical analogs; they contain the same information as Bode plots, but can be easier to interpret [3]. Our second method presents symbolic expressions for the effective stiffness and damping transmitted to the operator at low frequencies for a mass-damper-spring environment: Equations (8) and (9), respectively. We feel these symbolic equations are particularly elucidating and useful for design. Our analysis shows that:

- Local and communication time delay do not significantly affect the effective stiffness, strongly affect effective damping, and weakly affect effective mass transmitted to the operator. Local and communication and time delay have contrasting effects (e.g., local time delay *reduces* damping and communication time delay *increases* damping).
- For typical system parameters, low pass filtering has a small effect on the impedance transmitted to the operator.
- Increasing controller stiffness increases the effective stiffness transmitted to the operator at low frequencies, but can significantly change the effective stiffness, damping, and mass, at higher frequencies.

II. System Model

In this section we introduce the system model for a human interacting with a 1-degree-of-freedom (1-dof) impedance-impedance bilateral teleoperator. The system model (Figure 1), is used to generate the theoretical closed-loop impedance transmitted to the human, Z_{to}, as a function of system parameters.

The master teleoperator robot is modeled as a mass, m_m, with viscous damping, b_m,

$$Z_m = m_m s + b_m. \tag{1}$$

The slave teleoperator robot is modeled similarly, with mass, m_s, and viscous damping, b_s,

$$Z_s = m_s s + b_s. \tag{2}$$

The environment is modeled by a second-order system described by mass, m_e, viscous damping, b_e, and stiffness, k_e,

$$Z_e = m_e s + b_e + \frac{k_e}{s}. \tag{3}$$

We consider a position exchange proportional derivative controller with proportional gain K, and derivative gain B. The derivative gain is low-pass filtered with a cut-off frequency of ω_0 (rad/s). All individual control law blocks from Figure 1 (b), which map master or slave velocity to master or slave force, have the same form, $C_m = C_s = C_{ms} = C_{sm} = C$, where

$$C = \frac{K}{s} + \left(\frac{\omega_0}{s+\omega_0}\right) B. \tag{4}$$

We model two types of time delay: local time delay, t_d^{loc}, and communication time delay, t_d^{com}. Local time delay describes the time delay on commanded master forces from master position, or commanded slave forces from slave position, and models: (1) the fact that control is performed through a computer containing analog to digital, A/D, and digital to analog, D/A, components, resulting in a time delay of half the sample time on average, and (2) time delay due to amplifier dynamics. Communication time delay, t_d^{com}, describes the time delay on commanded master forces from slave position, or master forces from slave position. It models the same effects as local time delay, plus additional time delay from the communication channel. In many cases, communication time delay is much larger than local time delay because of physical distance.

We consider three environment conditions as follows.

Free $Z_e = 0$ **:** The slave robot is not in contact with the environment, $m_e = b_e = k_e = 0$.

Contact $Z_e = m_e s + b_e + k_e/s$ **:** The slave robot is in contact with an environment.

Clamped $Z_e \to \infty$ **:** The slave robot is rigidly clamped to the environment, $m_e, b_e, k_e \to \infty$.

III. Effect of System Parameters on Effective Impedances of Z_{to}

In this section, we analyze the impedance transmitted to the operator using two different methods. Our first method shows Z_{to} numerically using effective impedance plots for different local and communication time delays, low-pass filter cut-off frequencies of the velocity estimate, and controller stiffnesses, for different environment conditions. Our second method presents symbolic equations for the effective stiffness and damping transmitted to the operator at low frequencies. Using the block diagram in Figure 1(b), the closed-loop impedance transmitted to the operator can be derived:

$$Z_{to} = \frac{F_h}{V_h} = \frac{(Z_m + C_m d_l)(Z_s + C_m d_l + Z_e) + C_{ms} C_{sm} d_c^2}{Z_s + C_s d_l + Z_e}, \quad (5)$$

where

$$d_l = e^{-s t_d^{loc}}, \quad (6)$$

$$d_c = e^{-s t_d^{com}}, \quad (7)$$

and Z_m, Z_s, Z_e, are defined by Equations (1) - (3), respectively. In our analysis, we consider all controller blocks to have the same form given by Equation (4).

A. Numerical Effective Impedances of Z_{to}

Figure 2 shows the effective impedances of Z_{to} for various system parameters and environment conditions. The default system parameters are: $m_m = m_s = 100$, $b_m = b_s = 1$, $m_e = 250$, $b_e = 2$, $k_e = 250$, $K = 250$, $B = 2$, $\omega_0 = 100$, $t_d^{loc} = 0$, and $t_d^{com} = 0$, where mass is in g, damping in Ns/m, stiffness in N/m, frequency in rad/s, and time delay in s. These values were chosen to be representative of existing impedance-type master and slave robots [4], and teleoperator control system parameters for stability [5].

1) Effect of Local and Communication Time Delay: Local time delay, t_d^{loc}, and communication time delay, t_d^{com}, do not affect the effective stiffness, strongly affect the effective damping, and weakly affect the effective mass of Z_{to}.

Local time delay *reduces* effective damping, ED, and communication time delay *increases* ED; the amount subtracted or added per unit time delay is a function of controller and environment stiffness (see Equation 9). If both time delays are equal ($t_d^{loc} = t_d^{com}$), the ED of Z_{to} is reduced, except for the slave robot in free space ($Z_e = 0$), where the ED of Z_{to} is unchanged. In other words, the reduction in ED of Z_{to} from local time delay is larger than the addition of ED from communication time delay when the environment stiffness is non-zero. Figure 3 shows the change in effective damping transmitted to the operator at low frequencies as a function of controller and environment stiffness when the local and communication time delays are equal. Because the change in ED of Z_{to} scales with controller stiffness, K, small time delays can have a significant effect. For example, the effective damping transmitted to the operator at low frequencies when the slave robot is not in contact with the environment is increased 5 Ns/m for a teleoperator with $K = 500$ N/m, $t_d^{loc} = 0$ s, and $t_d^{com} = 0.005$ s.

Local and communication time delay weakly affect the effective mass, EM, transmitted to the operator: increasing local time delay *increases* effective mass, and increasing communication time delay *reduces* effective mass.

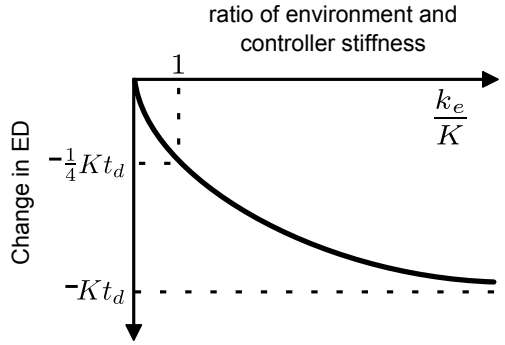

Fig. 3. The change in effective damping, ED, of Z_{to} per unit local and communication time delay as a function of the environment and controller stiffness ratio k_e/K. When the environment stiffness is zero, there is no net change ED for equal local and communication time delay, but as environment stiffness increases with respect to controller stiffness, the ED is reduced.

2) Effect of Low-pass Filter Cut-off Frequency: The low-pass filter of the velocity estimate, ω_0, affects the impedance transmitted to the operator differently depending on the environment impedance, Z_e. For the slave robot in free space ($Z_e = 0$), increasing the cut-off frequency increases the size of the ED and EM spikes of Z_{to}. For the slave robot in contact with the environment ($Z_e = m_e s + b + \frac{k_e}{s}$), or clamped ($Z_e \to \infty$), the cut-off frequency is the effective damping bandwidth of Z_{to}, i.e., the ED of Z_{to} is reduced for frequencies past ω_0.

3) Effect of Controller Stiffness : The controller stiffness, K, affects the impedance transmitted to the operator differently depending on the environment impedance. For the slave robot in free space ($Z_e = 0$), increasing controller stiffness increases the frequency range where Z_{to} is the sum of the master and slave dynamics: $Z_{to} = Z_m + Z_s$. For the slave robot clamped ($Z_e \to \infty$), the impedance of Z_{to} is similar to the sum of the master and controller dynamics: $Z_{to} = Z_m + C$. For the slave robot in contact with the environment ($Z_e = m_e s + b + \frac{k_e}{s}$), increasing K increases the transparency at low frequencies, and the high transparency bandwidth, but reduces transparency at high frequencies. Increasing K dramatically increases the effective stiffness, damping, and mass "spikes" transmitted to the operator.

B. Symbolic Low and High Frequency Effective Impedances of Z_{to}

The effective impedances of Z_{to} have a characteristic form: they are constant at low and high frequencies, and transition at "effective impedance bandwidths," e.g., the effective stiffness bandwidth. For a mass-damper-spring model of the environment ($Z_e = m_e s + b + \frac{k_e}{s}$), the effective stiffness, ES, and effective damping, ED, of Z_{to} at low frequencies are:

$$\bar{k} = \lim_{\omega \to 0} ES\{Z_{to}|_{Z_e = m_e s + b + \frac{k_e}{s}}\} = \frac{K k_e}{(K + k_e)}, \quad (8)$$

$$\begin{aligned} \bar{b} &= \lim_{\omega \to 0} ED\{Z_{to}|_{Z_e = m_e s + b + \frac{k_e}{s}}\} \quad (9) \\ &= b_m - B + \frac{2Bk_e(K + k_e) + K^2(B + b_s + b_e)}{(K + k_e)^2} \\ &\quad - K\left(1 + \frac{K^2}{(K + k_e)^2}\right) t_d^{loc} + 2K\left(1 - \frac{k_e}{(K + k_e)}\right) t_d^{com}. \end{aligned}$$

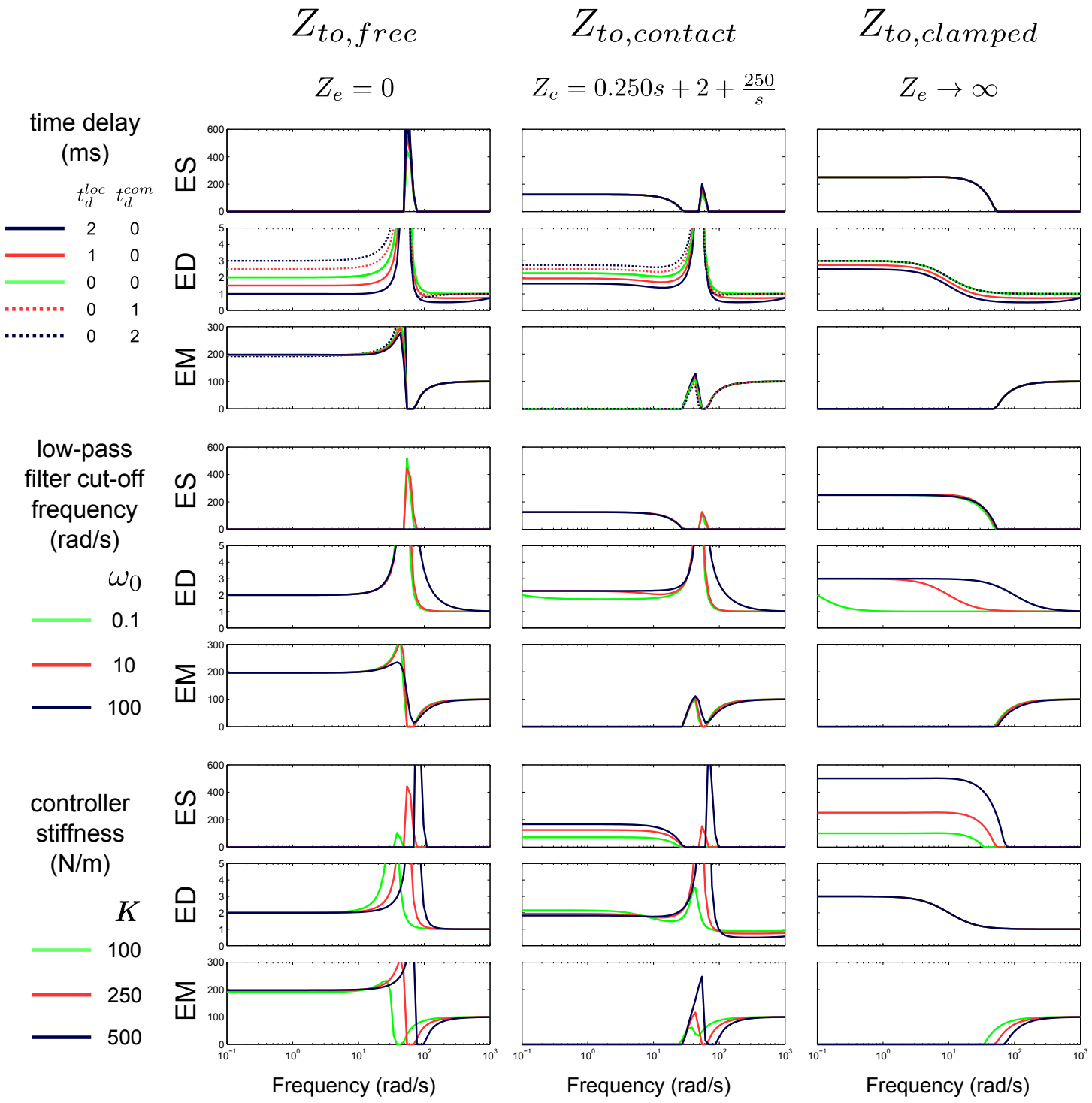

Fig. 2. Effective impedances of the impedance transmitted to the operator, Z_{to} for various system parameters and environment conditions. ES is the effective stiffness, ED is the effective damping, and EM is the effective mass. Local and communication time delay strongly affect the ED of Z_{to}: local time delay reduces ED, and communication time delay generally increases ED, except for a clamped environment ($Z_e \to \infty$), where communication time delay has no effect. The effect of the low-pass filter cut-off frequency on Z_{to} depends on the environment: for a free environment ($Z_e = 0$), it has little effect, for a clamped environment ($Z_e \to \infty$), the cut-off frequency determines the effective damping bandwidth. Increasing controller stiffness increases transparency at low frequencies, and the high transparency bandwidth, but reduces transparency at high frequencies due to larger effective impedance spikes.

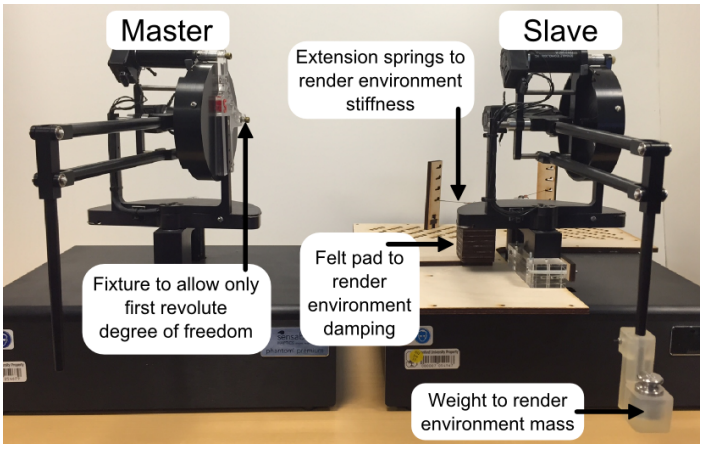

Fig. 4. The master (left) and slave (right) Phantom robots. Experiments were performed on the first revolute joints of the robots; the other joints were mechanically constrained by fabricated fixtures. The slave-side interaction environment consisted of dual extension springs for stiffness, a felt pad for damping, and a weight for mass.

The effective stiffness transmitted to the operator at low frequencies, $\bar{k}$, is a function of the environment stiffness and control stiffness; it corresponds to the equivalent stiffness of two springs in series, where one spring is the controller stiffness, and the other is the environment stiffness. Equation (8) is equivalent to "stiffness transparency" [8], which models the environment as a pure stiffness instead of a mass-damper-spring. It is always *less* than the environment stiffness k_e. As K increases, $\bar{k}$ become more similar to k_e; in the limit of infinite K, the effective stiffness transmitted to the operator equals the environment stiffness.

The effective damping transmitted to the operator at low frequencies, $\bar{b}$, is a function of master, slave, and environment damping, as well as controller stiffness and damping, environment stiffness, and local and communication time delay. Unlike the effective stiffness, $\bar{b}$ does not correspond to the equivalent damping of the controller and environment damping in series. The effective damping of Z_{to} can be smaller, or greater than, the environment damping b_e depending on systems parameters. In the limit of infinite control stiffness, $\bar{b} = b_m + b_s + b_e$.

IV. Experimental Impedances Transmitted to the Operator

Experiments were conducted with two Phantom robots and a constructed slave-side environment to compare experimental data to theoretical predictions (Figure 4). The experiments were performed on a single joint of the robots (the first revolute joint). The interaction environment consisted of dual extension springs for environment stiffness, k_e, a friction pad for environment damping, b_e, and an affixed mass for environment mass, m_e.

Two types of experiments were performed. The first set of experiments used system identification to find the master, slave, and environment, physical properties. The second determined the experimental closed-loop impedances transmitted to the operator.

A. System Identification of Master, Slave, and Environment

A system identification procedure was used to determine the properties (mass, viscous damping, and stiffness) of the master and slave Phantom robots and interaction environment.

The systems were excited with an exogenous chirp force with frequencies from 0.1 to 25 Hz and their position was measured. Velocity and acceleration signals were generated by numerical differentiation and smoothed with non-causal low-pass filters with no phase lag. Parameters $\hat{m}$, $\hat{b}$, and $\hat{k}$ were computed from the experimental data via optimization,

$$\hat{m},\hat{b},\hat{k} = \text{argmin} \sum (f_i - \hat{m}\ddot{x}_i - \hat{b}\dot{x}_i - \hat{k}x_i)^2 \qquad (10)$$

where f_i, $\ddot{x}_i$, $\dot{x}_i$, and x_i represent the signal values at a specific instant in time. Table I displays the system identification results averaged over five experiments for the master robot, slave robot, and environment. The correlation coefficient, r^2, is above 0.95 for all identified parameters, and the master and slave robot parameters are similar to those reported in [1] and [4].

TABLE I. System Fit Parameters

System	$\hat{m}$ (g)	$\hat{b}$ (Ns/m)	$\hat{k}$ (N/m)	r^2 (-)
Master	94	0.10	0	0.98
Slave	92	0.10	0	0.99
Environment	102	2.02	81	0.95

B. Experimental Impedances Transmitted to the Operator

An exogenous white noise input force excited the master robot for three minutes at a sample rate of 1 kHz. The impedance transmitted to the operator was computed by the ratio of the Fourier transform of the system's force and position, and then smoothed using a Hamming window. [7].

Figure 5 displays the experimental and theoretical Bode and effective impedance plots of Z_{to} for controller stiffness $K = 100$ (N/m), controller damping, $B = 2$ (Ns/m), and cut-off frequency $\omega_0 = 300$ (rad/s), with no added local communication or time delay. The experimental results are similar to theoretical predictions generated using Equation (5). Effective stiffness is near 45 N/m for frequencies smaller than 20 rad/s, and for greater frequencies, drops to zero. Effective damping at low frequencies is close to the predicted value given by Equation (9), "spikes" near 50 rad/s, and drops for frequencies greater than 100 rad/s. Effective mass is zero for frequencies less than 20 rad/s, and for greater frequencies, the experimental data is similar to the "hill-and-valley" shape predicted from the theoretical analysis.

Figure 6(a) displays experimental Z_{to} Bode and effective impedance plots for the same controller parameters as Figure 5, except with varying controller stiffnesses. This figure can be compared to Figure 2, which display the corresponding theoretical results. As predicted by the analysis, increasing controller stiffness increases the effective stiffness, but creates larger effective damping and effective mass spikes, transmitted to the human operator. In other words, the experimental data shows that increasing controller stiffness increases stiffness transparency at low frequencies, but significantly changes the effective damping and mass felt by the operator.

Figure 6(b) displays experimental Z_{to} Bode and effective impedance plots for the same controller parameters as Figure 5, except with varying communication time delay. This figure can be compared to Figure 2, which display the corresponding theoretical results. As predicted by theory, increasing communication

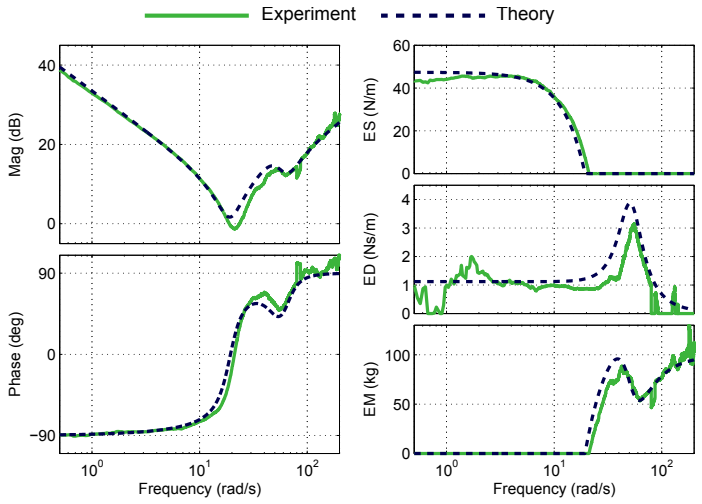

Fig. 5. Theoretical and experimental Bode and effective impedance plots of the impedance transmitted to the operator. ES is the effective stiffness, ED is the effective damping, and EM is the effective mass. The experimental data are similar to theoretical predictions generated using Equation (5).

time delay increases the effective damping, reduces the effective mass, and does not significantly change the effective stiffness, transmitted to the operator. In other words, the experimental data shows that increasing communication time delay does not affect the effective stiffness felt by the operator, but significantly changes the effective damping and mass felt by the operator.

V. Discussion

Increasing controller stiffness increases transparency at low frequencies, but can reduce transparency at high frequencies due to large effective damping and mass "spikes." This presents an interesting trade-off for designing the controller stiffness.

Our analysis shows that the effective stiffness transmitted to the operator is always less than the true environment stiffness. However, the effective damping can be substantially higher, or lower, than the environment damping. Equation (9) serves as a design tool to choose system parameters to achieve high damping transparency. Although the damping transmitted to the operator is a function of many system parameters, local and communication time delay have the strongest effect.

We show that local and communication time delay have a large effect on the impedance transmitted to the operator: the time delays strongly change the effective damping, weakly change the effective mass, and do not significantly change the effective stiffness. Because local and communication time delay have opposite effects on Z_{to}, e.g., local time delay decreases effective damping while communication time delay increases it, it is possible to offset the effect of local or communication time delay by artificially delaying the other. Of course, because both local and communication time delay can be destabilizing, a finite of time delay can be added.

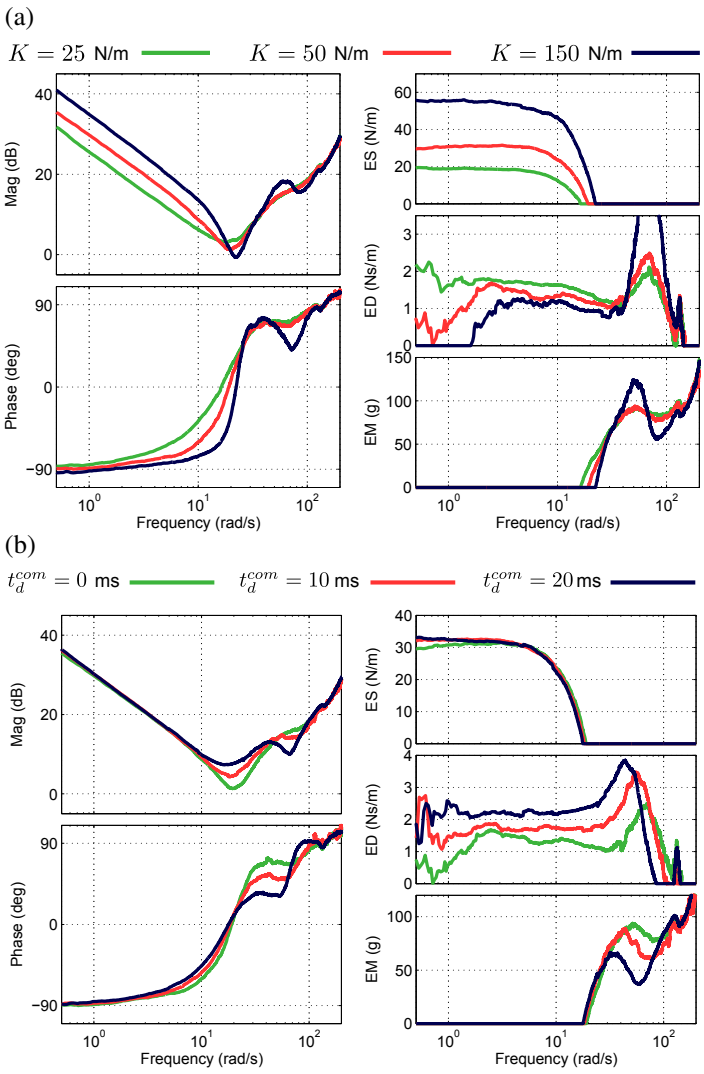

Fig. 6. Experimental Bode and effective impedance plots of the impedance transmitted to the operator. ES is the effective stiffness, ED is the effective damping, and EM is the effective mass. (a) As predicted from theoretical analysis (see Figure 2), increasing controller stiffness increases ES, but creates larger ED and EM spikes. (b) As predicted from theoretical analysis (see Figure 2), increasing communication time delay increases ED, and reduces EM, but does not significantly affect ES.

References

[1] M. Cavusoglu, D. Feygin, and F. Tendick. A critical study of the mechanical and electrical properties of the phantom haptic interface and improvements for high performance control. *Presence*, 11:555–568, 2002.

[2] G. A. V. Christiansson and F. C. T. Van Der Helm. The low-stiffness teleoperator slave – a trade-off between stability and performance. *International Journal of Robotics Research*, 26(3):287–299, 2007.

[3] N. Colonnese, A. F. Siu, C. M. Abbott, and A. M. Okamura. Rendered and characterized closed-loop accuracy of impedance-type haptic displays. *IEEE Transactions on Haptics*, 8(4):434–446, Oct 2015.

[4] N. Diolaiti, G. Niemeyer, F. Barbagli, and J. K. Salisbury. Stability of haptic rendering: Discretization, quantization, time delay, and coulomb effects. *IEEE Transactions on Robotics*, 22(2):256–268, 2006.

[5] K. Hashtrudi-Zaad and S. E. Salcudean. Analysis of control architectures for teleoperation systems with impedance/admittance master and slave manipulators. *The International Journal of Robotics Research*, 20(6):419–445, 2001.

[6] D. Lawrence. Stability and transparency in bilateral teleoperation. *IEEE Transactions on Robotics and Automation*, 9(5):624–637, 1993.

[7] L. Ljung. *System identification: theory for the user*. Prentice Hall, Upper Saddle River, NJ, USA, 1999.

[8] B. Willaert, D. Reynaerts, H. Van Brussel, and E. Vander Poorten. Bilateral teleoperation: Quantifying the requirements for and restrictions of ideal transparency. *Control Systems Technology, IEEE Transactions on*, 22(1):387–395, Jan 2014.